Chinese Chemical Letters 35 (2024) 108800

Contents lists available at ScienceDirect

Chinese Chemical Letters

journal homepage: www.elsevier.com/locate/cclet

Deactivation mechanisms and anti-deactivation strategies of molecular sieve catalysts for NO_x reduction

Fuli Wang[1], Penglu Wang[1], Jin Zhang, Dengchao Peng, Mengmeng Wei, Dengsong Zhang*

School of Environmental and Chemical Engineering, State Key Laboratory of Advanced Special Steel, International Joint Laboratory of Catalytic Chemistry, College of Sciences, Shanghai University, Shanghai 200444, China

ARTICLE INFO

Article history:
Received 13 March 2023
Revised 19 June 2023
Accepted 11 July 2023
Available online 14 July 2023

Keywords:
Environmental catalysis
NO_x reduction
Molecular sieve catalysts
Deactivation mechanism
Anti-deactivation

ABSTRACT

Molecular sieve catalysts, owing to their unique chemical properties, are widely used as catalysts among various catalytic reactions. Abundant Brønsted acid sites in molecular sieve catalysts usually enable active components to disperse well on the catalyst surface, and help to adsorb a large number of gas molecules to achieve maximum catalytic performance. Therefore, a variety of molecular sieve catalysts have been developed and used in the selective catalytic reduction of NO_x by NH_3 (NH_3-SCR). For example, Cu molecular sieve catalysts such as Cu-SSZ-13 and Cu-SAPO-34 with wide temperature windows and stable structure are considered and applied as commercial catalysts for NO_x removal in diesel vehicles for a long time. Although molecular sieve catalysts possess many advantages, they still cannot avoid the serious deactivation caused by various factors in practical applications. In this review, reasons leading to the deactivation of molecular sieve catalysts for NO_x reduction in actual working conditions were concluded. The deactivation mechanisms of molecular sieve catalysts for NO_x reduction were analyzed and the corresponding anti-deactivation strategies were summarized. Finally, challenges and prospects of molecular sieve catalysts for NO_x reduction were also proposed.

1. Introduction

Nitrogen oxide (NO_x, including NO and NO_2) is still one of main atmospheric pollutants at present. Its large emission could result in environmental pollution like acid rain and photochemical smog [1–8]. In addition, it can affect human health and cause some respiratory diseases [9,10]. To control the emission of NO_x from stationary or mobile source, many NO_x removal ($deNO_x$) technologies have been developed. Selective catalytic reduction of NO_x by NH_3 (NH_3-SCR) for both mobile and stationary sources is the most effective technology to control NO_x emissions [11–18]. Catalyst is the core of this technology, scientists have been working on to develop and improve more effective NH_3-SCR catalysts in recent years, which mainly be classified as metal oxide catalysts, noble metal catalysts, transition metal catalysts and molecular sieve catalysts (Fig. 1) [19–21].

Among various kinds of SCR catalysts, molecular sieve catalysts are always one of hotspots in research. Molecular sieve catalyst is a kind of crystalline silicate or silicon aluminate, with regular pore structures, mainly formed by oxygen-bridge bonds connected silicon oxygen tetrahedron or aluminum oxygen tetrahedron [22–24]. According to the different structure of molecular sieve catalysts, it can be divided into CHA type [25,26], LTA type [27,28], FAU type [29–31], MFI type [32–36], AEI type [37–41] and so on. Molecular sieve catalysts can ion-exchange with metal ions due to its unique structure and abundant Brønsted acid sites so that active components are dispersed highly in aluminosilicate. Because of its large specific surface area, molecular sieve catalysts are also exhibited its huge potential to act as a promising catalyst carrier. Therefore, they have been widely used in the study of NH_3-SCR catalysts. Table S1 (Supporting information) enumerates some typical NH_3-SCR molecular sieve catalysts. Some molecular sieve and metal oxide composite catalysts that reported in NH_3-SCR [38,42-45], are also listed in the Table S1. Among them, commercial catalysts like Cu-SSZ-13 and Cu-SAPO-34 are widely used in mobile sources, and researchers have conducted a lot of research on two catalysts [46–50]. Raquel *et al.* found that Cu-SSZ-13 can be synthesized by the one-pot method using copper-tetraethyl pentamethylene complex and *N,N,N*-trimethyl-1-adamant ammonium as organic structure directing agent (OSDAs) [51]. Xiao *et al.* found that Cu-SAPO-34 catalysts synthesized by direct ion exchange method (DIE) can separate more content of isolated Cu^{2+} and surface Cu, so its activity under low temperature is better than that of Cu-SAPO-34 synthesized by the conventional multistep ion

* Corresponding author.
E-mail address: dszhang@shu.edu.cn (D. Zhang).
[1] These authors contributed equally to this work.

https://doi.org/10.1016/j.cclet.2023.108800
1001-8417/

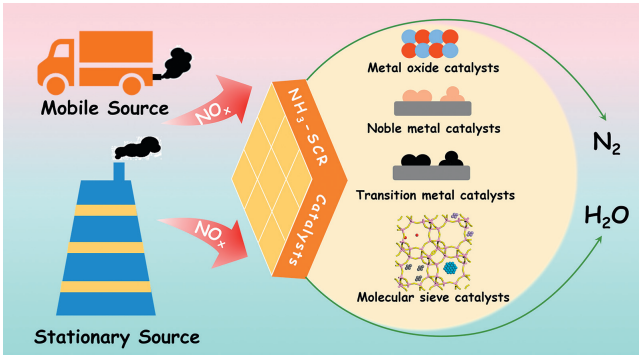

Fig. 1. Schematic of NO_x emission sources and the main kinds of NH_3-SCR catalysts.

exchange method [52]. And different types of copper species on Cu-SAPO-34 and Cu-SSZ-13 can be identified by combining IR spectroscopy and theoretical calculations [53]. In addition, there are many other types of molecular sieve catalysts used in NH_3-SCR. Yuan *et al.* developed a direct hydrothermal method by using a ferric complex, *i.e.* ethylenediaminetetraacetic acid ferric sodium (EDTA-FeNa), as both an iron source and a structure-directing agent, in which Fe/ZSM-5 molecular sieves showed significant NH_3-SCR activity. Under simulated industrial conditions, the conversion of NO_x is more than 99% in a wide temperature range of 573–693 K. At the same time, Fe/ZSM-5 molecular sieve also has good stability and tolerance to water vapor and sulfur dioxide, making these Fe/ZSM-5 zeolites promising candidates for practical application [54]. Naraki *et al.* proposed that Fe-BEA catalysts obtained by doping Fe into the beta molecular sieve framework had good performance for NH_3-SCR [55]. Zhu *et al.* believed that better NH_3-SCR performance of Fe-Beta was not affected by the specific structure, but because the layered Fe-Beta molecular sieve catalysts had more Fe active sites and could better disperse Fe species between layers [56]. Fully copper-exchanged high-silica LTA zeolites not only have good NH_3-SCR performance, but also own high hydrothermal stability [28,57]. Catalysts supported by molecular sieve catalysts or bimetal exchanged molecular sieve catalysts, such as MnO_x/SAPO-34 [58], CuNi/SSZ-13 [59], CuFe/ZSM-5 [60,61], also have good SCR activity.

Although molecular sieve catalysts have been reported to possess many advantages that guarantee their excellent SCR performance, there are still many factors that will cause the deactivation of catalysts in actual working conditions. Like metal oxidation catalysts, many researchers have thoroughly studied the poisoning mechanisms of alkali metals, heavy metals, phosphorus and SO_2, and even the multiple poisoning of K&Pb and Cd&SO_2 on common SCR catalysts, and put forward some corresponding anti-deactivation strategies to address these poisoning problems [21,62-65]. Similarly, hydrothermal aging and deactivation caused by sulfur poisoning are two difficult problems in the application of molecular sieve catalysts [45,66-74]. In addition, toxic deactivation caused by alkali metals, alkaline earth metals, phosphorus and HCl, *etc.* will also reduce the activity of molecular sieve catalysts and affect their service life [75–77]. Therefore, in addition to the catalytic activity of molecular sieve catalysts, their deactivation mechanism is also worthy of attention and research. Only when the deactivation mechanism of catalysts is clear, more effective anti-deactivation strategies can be proposed. Here we summarize the deactivation mechanisms of molecular sieve catalysts and some anti-deactivation strategies proposed by predecessors, hoping to give readers a better understanding in this research field (Fig. 2).

2. Deactivation mechanism and anti-deactivation strategies for hydrothermal aging

2.1. Deactivation mechanism for hydrothermal aging

Molecular sieve catalysts are often applied in motor vehicles, and the temperature of motor vehicle exhaust can be as high as 800 °C above, and the exhaust always has indefinite quantity water. Under this condition, the catalyst have to undergo hydrothermal aging, leading to the collapse of the framework and the agglomeration of active components, thus its activity will be reduced, and also its service life. At present, the stability of hydrothermal aging of molecular sieve catalysts is one of the important criteria for commercial application. Over the past decade, there were many reports on the hydrothermal aging of molecular sieve catalysts. Kwak *et al.* thermally aged four kinds of Cu-zeolite catalysts (Cu-beta, Cu-ZSM5, Cu-SSZ-13, Cu-Y) at 800 °C for 16 h. It was found that the aluminum coordination environment of Cu-ZSM-5 and Cu-β changed obviously, accompanied with Cu-aluminate species and CuO were found in two catalysts. And Cu-SSZ-13 is mainly reduced in redox capacity [78]. Young *et al.* analyzed the hydrothermal aging and deactivation mechanism of Cu-SSZ-13 under different Cu/Al and Si/Al conditions. It was found that the higher the Cu/Al, the more serious decrease of activity caused by hydrothermal aging [72]. Since the D6R (double-6-ring subunit) site was first

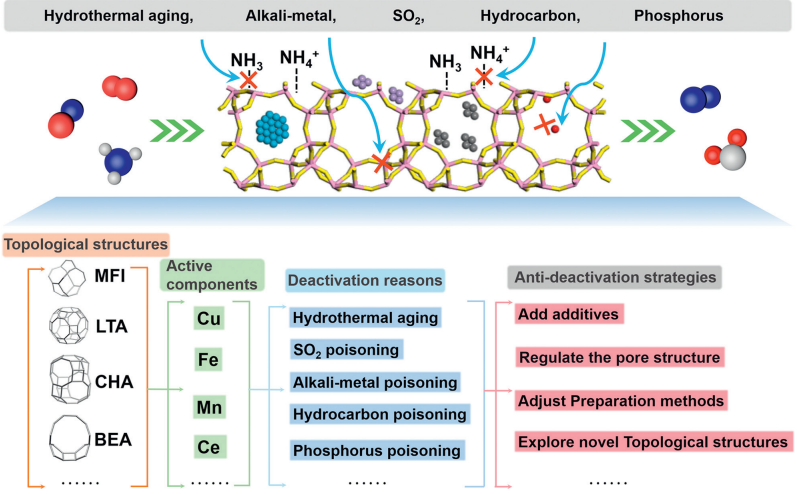

Fig. 2. Schematic of the types, active components, deactivation reasons and anti-deactivation strategies of molecular sieve catalysts.

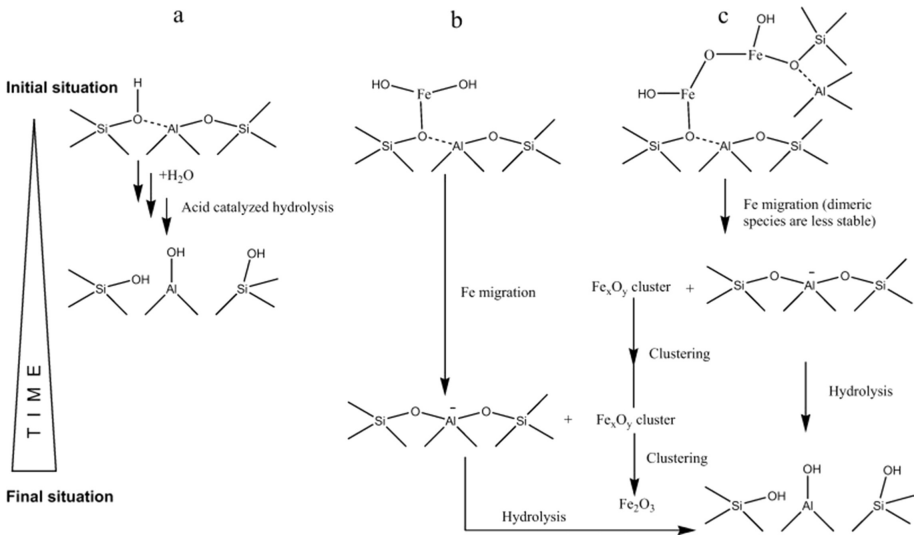

Fig. 3. Scheme of hydrothermal aging of (a) Brønsted-acid sites, (b) isolated iron sites and (c) dimeric iron sites involving dealumination, migration and clustering. Reproduced with permission [89]. Copyright 2011, Elsevier.

occupied by the Cu^{2+} ion, the CHA site also began to be occupied as Cu/Al ratio gradually increased. However, because of the unstable nature of Cu^{2+} on CHA sites, condensation was more likely to occur than Cu^{2+}, which led to the formation of CuO_x. Therefore, it was proposed that the main reason for the hydrothermal aging deactivation of Cu-SSZ-13 was the growth of CuO_x destroyed zeolite cages and pores, which led to the structure collapse. Other researchers believed that hydrothermal aging will lead to dealumination of Cu-SSZ-13 catalysts, resulting in the serious reduction of Brønsted acid sites and the crystallinity decrease. At the same time, the isolated $Al(OH)_3$ ion and Cu^{2+} ions combined to form $CuAlO_x$ species, which deactivated the Cu species [79–82]. However, there are different opinions on Cu-SAPO-34 about the hydrothermal aging. Su *et al.* showed that vacancies in the framework of SAPO-34 caused by desilication can be repaired by migration of Al and P atoms outside the framework to defects. After aging, active Cu species in Cu/SAPO-34 zeolites tend to accumulate, which enhanced the redox ability and maintained its acidity [83]. But some studies have shown that dealumination, Cu^{2+} migration and weakening of acidity can occur both in Cu-SAPO-34 and Cu-SSZ-13 after hydrothermal aging, leading to the decline in NH_3-SCR performance [79]. Fan *et al.* found that after aging at 950 °C for 3 h, the crystallinity of SAPO-34 began to decrease. After 6 h, the zeolite crystals began to transition to SiO_2 and $AlPO_4$ phases. Meanwhile, the Si-OH-Al bond was broken, the Brønsted acid site and Cu^{2+} species were reduced. And the higher the Cu loading, the more obvious the Si-OH-Al bond breakage [84,85]. Furthermore, Wang *et al.* found that after hydrothermal aging (at 700 °C in 10 vol% H_2O/air for 48 h), CuO_2 species on the Cu-SAPO-34 surface would be transferred to the ion exchange site, thus improving the activity of the catalyst at 200–260 °C. But in general, hydrothermal aging usually causes Cu-SAPO-34 to lose a large amount of acidity [86,87]. Peter *et al.* showed the change process of catalyst structure after aging of Cu-ZSM-5 and Cu-IM-5 catalysts: (1) partial dealuminization of molecular sieve, (2) reversible migration of Cu species, (3) forming some inactive or stable Cu-Al clusters (Fig. S1 in Supporting information). They also indicated that the stability of Al in the framework had great influence on the properties of Cu-ZSM-5 and Cu-IM-5 catalysts after hydrothermal aging [88].

The causes of hydrothermal aging deactivation of Fe/zeolite catalysts have also been investigated: (I) the facile dealumination of Al-OH-Si sites, (II) the fast loss of dimeric iron active sites, and (III) tardy migration of isolated iron ions after dealumination [89]. Fig. 3 showed the general scheme for dealumination, migration and aggregation of Fe-ZSM-5 catalysts after the process of hydrothermal aging. The hydrothermal aging deactivation of Fe/BEA, Fe/SSZ-13 and other Fe/zeolite catalysts also follows mechanisms such as dealumination and Fe species change [90–92]. Iwasaki *et al.* also found that the decreasing order of SCR performance of several Fe molecular sieve catalysts is: Fe-BEA > Fe-MFI > Fe-FER > Fe-LTL > Fe-MOR (Fig. S2 in Supporting information). The activity of each catalyst decreased after hydrothermal aging, and the order of activity was as follows: Fe-MFL > Fe-BEA > Fe-FER > Fe-LTL > Fe-MOR. Therefore, the degree of deactivation caused by hydrothermal aging also depends on the ratio of silicon to aluminum [93]. For dual-active molecular sieve catalysts such as CuFe/BEA, hydrothermal aging can also inhibit the formation of active oxygen vacancies and charge transfer between Cu and Fe [94].

In summary, the effect of hydrothermal aging on molecular sieve catalysts can be divided into three parts: (1) affect the framework of molecular sieve catalysts; (2) affect active components; and (3) affect the surface properties of catalyst such as acidity and redox ability. The active sites, acidity and redox ability of catalysts are closely related to the NO_x reduction ability, hence, hydrothermal aging will lead to the decrease of the activity of molecular sieve catalysts.

2.2. Anti-deactivation strategies for hydrothermal aging

In order to solve the aging deactivation problem of molecular sieve catalysts, some anti-deactivation strategies have been proposed and shown as following.

(1) Improve the stability of the catalysts by adding additives. Iwasaki *et al.* proposed earlier that rare earth elements (rare earth metals with trivalent cation radii of 1.05–1.15 Å) can inhibit dealumination and lead to the formation of terminal silanol and iron oligomer, so that Fe/BEA catalyst can maintain good NH_3-SCR activity after hydrothermal aging (at 973 K for 5 h under 3% H_2O/air condition) [95]. Subsequently, it was found that introducing a small amount of Ce or Y rare metals into Cu-SSZ-13 or Cu/SAPO-34 molecular sieve catalysts by using ion exchange method can improve the stability of the framework and active centers, so as to ensure the SCR activity and anti-aging ability [96–99]. And also, Deng *et al.* believed that Ce doping was not

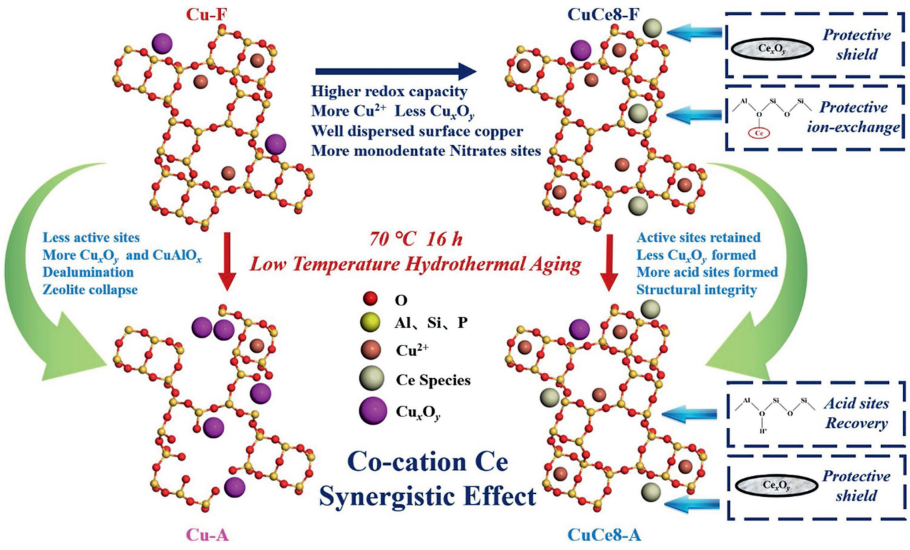

Fig. 4. Promotional effect and mechanism of the modification of Ce on the NH_3-SCR performance and the hydrothermal stability of Cu/SAPO-34 catalysts. Reproduced with permission [102]. Copyright 2021, Elsevier.

only conducive to the formation of aluminum framework, but also helped stabilize the framework and Cu active centers, and improved the hydrothermal stability of catalysts. Chen *et al.* concluded that La ions incorporating into Cu-SSZ-13 can improve its hydrothermal stability when the optimal La content for Cu_4-La-SSZ-13 is ≤0.15 wt% [100]. However, with the La content increased, the framework aluminum and Cu active centers of Cu/SSZ-13 are reduced after hydrothermal aging, and even the CHA framework structure is destroyed, which is very unfavorable to the hydrothermal stability [101]. Similarly, Guan *et al.* also investigated that Ce species protected the copper ions and prevented the desalinization during aging over Cu/SAPO-34. After Ce doping, active copper sites and single dentate nitrate adsorption sites were greatly increased, thus improving SCR performance and stability (Fig. 4) [102].

Other studies have shown that hydrothermal stability of Cu-SAPO-34 catalysts at low temperature can also be improved by adding noble metal Ag [103]. In addition, alkali metal Na or Li can also be introduced into the framework of molecular sieve catalysts as an additive to improve their hydrothermal stability. This is owing to the fact that alkali metal ions could occupy a part of Brønsted acid sites, which slows down the framework hydrolysis during hydrothermal aging process and improves their hydrothermal stability (Fig. S3 in Supporting information) [76,104]. Phosphorus was often used as a non-metallic element that can poison nitrogen oxide purification catalyst, but Zhao *et al.* found that the addition of a certain amount of P was conductive to the hydrothermal stability of Cu-SSZ-13. After hydrothermal treatment with the same method, the SCR activity of P-Cu-SSZ-13 remained at a very high level, while Cu-SSZ-13 was close to deactivation. This is due to the addition of P obtains the silicon-aluminum phosphate interface in the framework of zeolites (Fig. S4 in Supporting information), which weakens the dealumination in the framework after hydrothermal aging, thus improving the hydrothermal stability [105]. Wang *et al.* added the anions SO_4^{2-}, NO_3^- and Cl^- as additives to the mesoporous MCM-48 zeolite catalysts, and found that these anions all improved the hydrothermal stability of molecular sieve catalysts, of which SO_4^{2-} had the best effect [106]. Tian *et al.* used atomic layer deposition (ALD) to coat the surface with a stable layer of nano-SiO_2 to improve the hydrothermal stability of Cu-SSZ-13. After aging for 16 h under 800 °C with 12.5% water, SiO_2 coating can still avoid inactivation by inhibiting the alumina leaching in SSZ-13. Moreover, SiO_2 nanolayer is so thin that it neither block zeolite pores nor affects the NO_x reduction ability of Cu-SSZ-13 [107]. Therefore, it can be considered that adding additives is one of the methods to solve this problem.

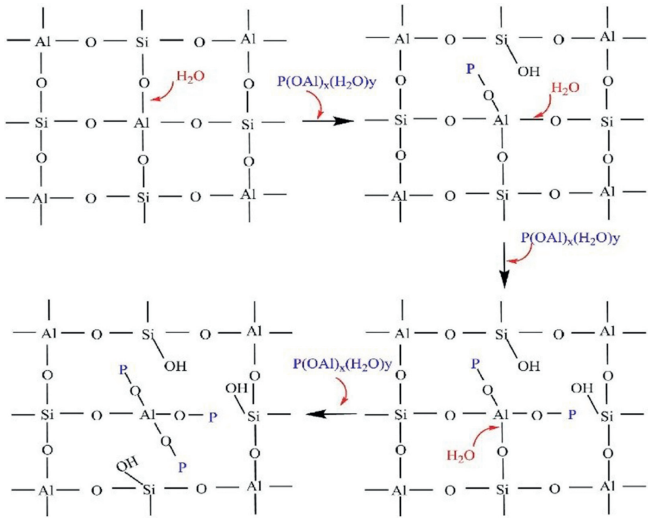

Fig. 5. Schematic illustration of the structural stability of Cu-SSZ-13 enhanced by extra-framework P atoms from SAPO-34 in the mixed sample. Reproduced with permission [109]. Copyright 2020, Elsevier.

(2) Optimize the preparation or treatment methods of catalysts. Jiang *et al.* proposed that Cu-SSZ-13 prepared by ion exchange method had higher resistance to hydrothermal aging than that prepared by one-pot method [108]. Ma *et al.* reported that Cu-SSZ-13 and Cu-SAPO-34 had a strong synergistic effect and the existence of Cu-SAPO-34 could enhance the hydrothermal stability of Cu-SSZ-13 (Fig. 5) [109]. Moreover, it can be found that the Cu-zeolite catalysts prepared by SAPO-34 instead of the traditional SSZ-13 microcrystal can yield higher performance as the crystal seed was inhibited during hydrothermal aging process, and the isolated Cu^{2+} site remained almost unchanged [110]. Wang *et al.*

obtained mesoporous MCM-48 zeolite catalysts with better hydrothermal stability by carefully adjusting the synthesis conditions [111]. Therefore, the selection of the best preparation method and the best crystal seed can improve the possibility of obtaining the catalyst with high hydrothermal stability. Some optimized treatment of zeolite catalysts can also improve the hydrothermal stability. Huang *et al.* made Cu-SAPO-34 catalysts using the same composition but different crystal seed sizes (1–13 μm) by one-pot synthesis. It was found that smaller crystal seed size of the fresh catalyst induces less Si-O-Al structures on the surface, and less affected by water vapor hydrolysis, and less damage to the molecular sieve structure after long-term hydrothermal aging at low temperature, that is, higher the hydrothermal stability (Fig. S5 in Supporting information) [112]. Zhang *et al.* used ammonium hexafluoro silicate (AHFS) to modify Cu-SSZ-13 and reported it possessed the enhanced hydrothermal stability. After hydrothermal treatment at high temperature, the AHFS treated Cu-SSZ-13 still kept the CHA structure stably and the original activity was remained to a large extent, while the CHA structure of the contrast sample had collapsed and some of the active Cu^{2+} ions had been transformed into low active CuO, which greatly reduced the activity [113]. Zhang *et al.* improved the hydrothermal stability of Cu-ZSM-5 by modification of surface [114]. Chen *et al.* applied co-templates with tetraethylammonium hydroxide and copper-tetraethylenepentamine to synthesis the nanosized Cu/SAPO-34. Compared with conventional Cu/SAPO-34 catalysts, the as-prepared catalysts had the enhanced NH_3-SCR activity and the hydrothermal stability [115]. Wang *et al.* discussed that the increase of P/Al ratio can not only improve the crystallinity of the catalyst, but also increase the grain size, which is beneficial to the stability of the zeolite framework. Cu-SAPO-34 with large grain size owns the advantage of promoting the transformation of CuO into isolated Cu^{2+} ions and inhibits the aggregation of Cu species. In addition, the catalyst with a larger grain size also provides more acid sites, so that the catalyst possesses the good hydrothermal stability (Fig. S6 in Supporting information) [116].

(3) Adjust the pore structure of molecular sieve catalysts. Pu *et al.* found that MSAMS-2 and MSAMS-4 which are belong to SBA-15-type mesoporous aluminosilicates had small, stable five-element ring subunits that effectively prevented the attack of water molecules, so this type of mesoporous zeolite catalyst had good hydrothermal stability [117]. In addition, mesoporous ZrMCM-48 zeolite catalysts, mesoporous V-MCM-41 molecular sieve catalysts and mesoporous MCM-48 molecular sieve catalysts have high hydrothermal stability [118–120]. Xu *et al.* obtained highly hydrothermal stable mesoporous molecular sieves by ZSM-5 desilication [121]. Luo *et al.* prepared mesoporous aluminosilicate molecular sieve catalysts with high hydrothermal stability by diluted ZSM-5-type precursor with mesoporous MCM-41 [122]. In addition, the stable ordered mesoporous aluminosilicate catalysts (MASMS-1) can be obtained in high temperature steam by using ZSM-5 as precursor assembled with mesoporous MCM-41 [123]. Moreover, some researchers propose that the most promising method to strengthen the hydrothermal stability of mesoporous aluminosilicate is to construct mesoporous structures by using nano-clusters of aluminosilicate zeolite as raw materials [124]. Therefore, it is believed that the hydrothermal stability can be modulated *via* adjusting the pore structure of molecular sieve catalysts.

(4) Search for a new molecular sieve catalyst with high hydrothermal stability. There are many kinds of molecular sieve catalysts. At present, molecular sieve catalysts commonly used in SCR are only a small part of them, and there are many other types of molecular sieve catalysts waiting for researchers to explore. Moliner *et al.* synthesized the copper-exchanged SSZ-39 molecular sieve for the first time [125]. The main component of SSZ-39 (AEI) is silico-aluminate and it has a three-way pore system (8-R) with large cavities of D6R in the structure. The molecular sieve catalyst can keep Cu^{2+} stable in the test, avoid dealuminization and copper migration, and had good catalytic performance. Shan *et al.* compared the NO_x reduction performance of Cu-SSZ-39 and Cu-SSZ-13 before and after hydrothermal aging (Fig. S7 in Supporting information). It was found that Cu-SSZ-39 catalysts still maintained considerable activity after aging, which was due to the more stable framework aluminum and Cu^{2+}, resulting in high hydrothermal stability [126]. There are some other types of molecular sieve catalysts, such as high-silica LTA zeolites, high-silica ERI zeolite, EU-7 zeolite, USY zeolite and nano-CHA zeolite, which have also been proved to have high hydrothermal stability [57,127-132]. Therefore, the design for new type of molecular sieve catalysts is also a promising direction for enhancing the hydrothermal stability.

3. Deactivation mechanism and anti-deactivation strategies for SO_2 poisoning

3.1. Deactivation mechanism for SO_2 poisoning

Sulfurous compound is often contained in fuel and engine oil, leading to the production of SO_2 in the exhaust gasses [133]. Therefore, the introduction of gaseous SO_2 is mainly used to simulate sulfur poisoning in the research. Sulfur poisoning mainly affects the NO_x reduction activity and durability of catalysts, especially Cu molecular sieve catalysts. Peter *et al.* exposed Cu-CHA catalysts to SO_2 and found that SO_2 can cause irreversible deactivation, thus affecting the service life of catalysts [134]. William *et al.* treated Cu-CHA catalysts by sulfurization and found the specific surface area after sulfurization reduced by 20%. Moreover, active Cu sites in catalysts could be severely hindered, leading to the decreased absorption of NO_x [135]. Besides, the presence of ammonium sulfate was found in the sulfurized samples, and ammonia sulfate covered the surface of the catalyst, which also affected the activity. Su *et al.* have studied the sulfur species on the surface of sulfur-poisoned Cu-CHA catalysts and found that H_2SO_4, $CuSO_4$ and $Al_2(SO_4)_3$ species deposited on the surface, which indicates that sulfur has an effect on both the active center and the framework of molecular sieve catalysts [136]. It had also been shown that copper bisulfate species would be produced in the sulfur poisoned Cu-CHA catalysts [137]. Hammersh and Shih *et al.* studied the specific sites of Cu-CHA who interacted with SO_2, and found that SO_2 mainly interacted with Z-CuOH sites which contained a framework aluminum center, that is, Z-CuOH site was more prone to SO_2 deactivation than Z_2Cu site (Fig. S8 in Supporting information) [138,139].

In order to further explore the toxicity of sulfur poisoning to molecular sieve catalysts and clarify the deactivation mechanism of sulfur poisoning, a single molecular sieve catalyst was selected for more detailed study. Sandra *et al.* explored the impact of SO_2 on Cu-SSZ-13 at different temperature and found that SO_2 caused serious deactivation of the catalyst at lower temperature (220 °C), while SO_2 had little effect on Cu-SSZ-13 catalysts at higher temperature (400 °C) and SO_2 would also reduce the selectivity of catalyst for N_2 [140]. Ammonium sulfate was mainly formed at about 200 °C, while copper sulfate was mainly produced after sulfur poisoning at 400 °C, which indicated that ammonia sulfate species had a great influence on the NO_x reduction ability of molecular

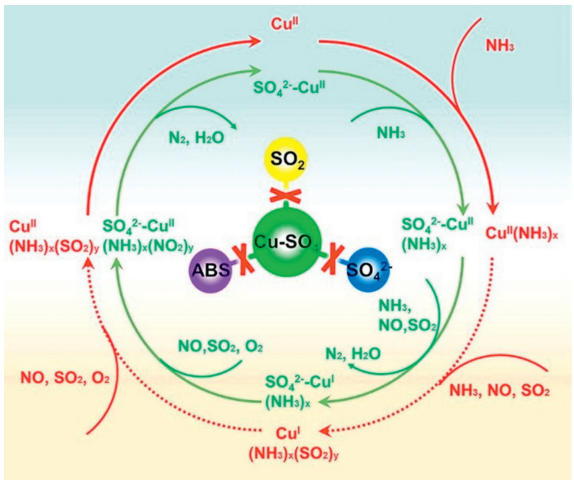

Fig. 6. Schematic illustration of the standard SCR reaction cycle for different Cu-SAPO-34 catalysts in the presence of SO_2. The dash line indicated that the reaction process was inhibited. Reproduced with permission [153]. Copyright 2022, Elsevier.

sieve catalysts [141]. Kurnia *et al.* found that under SCR conditions (NH_3 + NO + O_2 + H_2O), the available copper sites in the redox cycle were reduced after SO_2 poisoning due to occupation by ammonium sulfur species, indicating that sulfur poisoning could significantly reduce the catalytic activity of molecular sieve catalysts by reducing the redox capacity [142]. For another commercial catalyst of Cu-SAPO-34, after sulfur poisoning, sulfates formed after sulfur poisoning also result in greatly reduced specific surface area and pore volume. In more details, some pores among Cu-SAPO-34 are blocked, active Cu sites that can participate in the redox cycle were rapidly decreased which had significant effect on the standard SCR reaction [143–145]. However, a slight difference with Cu-SSZ-13 is that SO_2 is difficult to interact with H-SAPO-34, so SO_2-poisoning hardly affected the crystallinity and characteristic structure [146].

In general, the SO_2 deactivation mechanism of Cu-SAPO-34 can be summarized as follows: (1) SO_2 may attack isolated Cu^{2+} to form copper sulfate/sulfite species, causing the active Cu^{2+} species to lose the ability to participate in the reaction; (2) competitive adsorption of SO_2 and NO_x, and (3) ammonium sulfate covers active sites and pores are blocked [147–150]. Other types of molecular sieve catalysts, such as Cu-SSZ-39 with high hydrothermal stability, also cannot avoid the reduction in NH_3-SCR activity caused by sulfate coverage of active sites [151]. Therefore, the improvement of sulfur resistance of molecular sieve catalysts is also an important direction in the research of catalysts.

3.2. Anti-deactivation strategies for SO_2 poisoning

At present, some effective anti-deactivation strategies for sulfur poisoning of molecular sieve catalysts have been proposed. Liu *et al.* reported, the Cu-SAPO-34 catalysts synthesized by ion exchange method had better sulfur resistance than that prepared by impregnation method, so it is believed that the preparation method can enhance the sulfur tolerance of molecular sieve catalysts [152].

He *et al.* studied SO_4^{2-}-coordinated Cu-SAPO-34 catalyst which can sustain the integral SCR reaction cycle after SO_2 poisoning. It is due to the reserved reduction and re-oxidation process of Cu species (Fig. 6) [153]. In addition, since Ce is easy to react with SO_2 to form hard-to-decompose $CeSO_4$ species, the researchers proposed to add Ce to molecular sieve catalysts as a sacrifice site to protect the active site and reduce the inactivation caused by sulfur poisoning. Fan *et al.* introduced Ce into the framework of SAPO-34 and found that Ce suppress the reaction of SO_2 over Mn-Ce/CeSAPO-34 catalyst to form NH_4HSO_4, and Ce is easier to interact with SO_2, thus retaining the activity of Mn centers [154]. Li *et al.* also observed a similar enhancement effect by doping Ce into Fe/Beta catalyst [155]. Li *et al.* coated CeO_2 over Cu-SAPO-18 catalysts and found that it could also achieve the purpose of improving sulfur resistance [156]. In addition to Ce, another rare earth element Pr had also been found to prevent the sulfurization of MnO_x/SAPO-34 catalyst and suppress the coating of ammonium sulfate upon catalysts (Fig. S9 in Supporting information) [157]. Yu *et al.* designed Cu-SSZ-13-$ZnTi_{10}O_x$ catalyst and it showed the great NH_3-SCR performance and had better anti-SO_2 poisoning ability compared to Cu-SSZ-13. $ZnTi_{10}O_x$, as a sacrificial component, may be preferentially poisoned by SO_2, resulting in the migration of Cu^{2+} from 8MR to 6MR which enhanced interaction with SSZ-13 support, thus improving SO_2 resistance [45]. These results indicated that adding additives can improve the tolerance of molecular sieve catalysts to SO_2.

On the other hand, in order to solve the problem of insufficient anti-SO_2 ability for Cu-ZSM-5 microporous molecular sieve catalysts, Peng *et al.* synthesized multistage porous Cu-ZSM-5–*meso* catalyst with both micropore and mesoporous structure. In contrast to the conventional Cu-ZSM-5 molecular sieve catalysts, the new molecular sieve catalyst had higher mesoporous mass transfer capacity, larger specific surface area, stronger acidity and NO adsorption ability, and had better NH_3-SCR activity and anti-SO_2 performance at medium and low temperature [158]. He *et al.* also recently found that constructing phobic Cu sites can alleviate SO_2 poisoning of Cu-SAPO-34 in NH_3-SCR *via* a hydrothermal aging (HA) method. After HA treatment, the adsorption capacity of SO_2 and deposition amount of ABS were reduced, and the overoxidation and polymerization of Cu species induced were also inhibited, thus maintaining the redox balance in NH_3-SCR reaction [159].

4. Deactivation mechanism and anti-deactivation strategies for alkali-metal poisoning

4.1. Deactivation mechanism for alkali-metal poisoning

Due to the increasing demand for energy and the decreasing number of fossil fuels, researchers have turned their attention to renewable energy. As a new type of green power plant fuel, biomass is widely distributed and has low carbon emission. Unlike typical fossil fuels, however, biomass contains much higher contents of alkali metals [160]. Though SCR units can be placed after the electrostatic precipitator of power plant, the exhaust gasses still contain certain contents of fly ash involving alkali and alkaline earth metals, which will produce toxic effects on SCR catalysts [161].

The exhaust gasses from vehicle sources is also reported to contain different content of alkali metals as generated from the combustion of oil, *etc.* Thus, molecular sieve catalysts applied both among stationery and vehicle sources are also inevitably affected by these toxic substances. Due to its larger specific surface area and stronger acidity, Cu-based molecular sieve catalysts have promoted tolerance to alkali/alkaline earth metal than commercial VW/Ti catalysts [162]. However, the SCR performance of Cu-based molecular sieve catalysts will be significantly affected when the toxic substance content is too high.

Alkali/alkaline earth metals that lead to molecular sieve catalysts poisoning generally include K, Na, Ca, Mg, *etc.* Putluru *et al.* exposed Cu-HZSM-5 and Cu-HMOR catalysts to KCl aerosol for a long time, and found that the catalysts were deactivated by 58% and 48% respectively [163]. Ma *et al.* found that when potassium content was high (>0.5%), the NO_x reduction ability of Cu-SAPO-34 significantly affected, and proposed that potassium poisoning would cause Cu^{2+} (the highest activity) to be transformed into

square-plane CuO/Cu_2O clusters (the lowest activity), causing the deactivation of Cu-SAPO-34 [164]. Liu *et al.* systematically investigated the toxic effects of various potassium salts such as K_2CO_3, K_3PO_4 and K_2SO_4 on Cu-SSZ-13. It was found that the diffusion of K^+ into molecular sieve catalysts and then can form Si-O (K)-Al by exchanging with H^+ and separated Cu^{2+} (Fig. S10 in Supporting information), leading to the decline of Brønsted acid sites and isolated Cu^{2+}, thus inhibited the NH_3 adsorption on the surface and destructed the catalytic activity of molecular sieve catalysts [165]. The toxic effect of Na^+ on Cu-zeolite catalyst is similar to that of K^+, and Na^+ will also conduct ion exchange with H^+ and Cu^{2+}in catalysts, resulting in the decrease of Cu^{2+} and acid center [166]. The toxic effect of alkaline earth metal Ca on catalyst is slightly different from that of alkali metal. Xue *et al.* loaded CaO on Cu/ZSM-5 and caused the decline of specific surface area and acid sites. Meanwhile, the interaction between CaO and CuO weakened the CuO reducing capacity, which will affect the activity of the catalyst [167]. The effects of K, Na, Ca and Mg on molecular sieve catalysts were compared. It was found that the toxic order of K, Na, Ca and Mg to Cu-SSZ-13 was Mg > Ca > Na > K, to Cu-SSZ-39 was K > Mg > Ca > Na, and to Cu-SAPO-18 was K > Na > Ca > Mg [168–170]. This shows that different kinds of molecular sieve catalysts have different degrees of tolerance to alkali/alkaline earth metals.

The alkali deactivation mechanism of Fe molecular sieve catalysts is mainly for the decrease of acidity and NH_3 storage capacity, but more important deactivation mechanism is that the pores are blocked by free poisons and/or the micropores are narrowed due to the adsorption of alkaline metals at cation sites [171]. Otherwise, alkali metals can generate the reduction of active Fe species in Fe zeolites. Liu *et al.* reported that more K deposition (>0.5%) occupies the Brønsted acid site of Fe/Beta catalyst, resulting in the accumulation of active Fe species, increasing the NO oxidation activation energy at Lewis acid sites, but also inducing the formation of inert nitrate, blocking pores of beta zeolite, and significantly reducing active Fe species [172]. The deactivation mechanism of alkali/alkaline earth metals on molecular sieve catalysts can also be summarized as: (1) the effects on the active species; (2) the effects on catalyst structure; and (3) the influence on acidity and oxidation reducibility of catalysts.

4.2. Anti-deactivation strategies for alkali-metal poisoning

According to the alkali-metal deactivation mechanism of molecular sieve catalysts, alumina-rich zeolites with rich Brønsted acids was developed to improve the exchange capacity of K^+ and protect isolated Cu^{2+} ions [173]. Moreover, the preparation of molecular sieve catalysts with core-shell structure is also a good method to improve the resistance to alkali metals. Liu *et al.* prepared Fe/Beta@meso–CeO_2 catalyst with core-shell structure, and found that this catalyst not only had excellent alkali resistance, but also had good sulfur toxicity resistance [174]. Chen *et al.* synthesized Cu/SSZ-13 by a simple method to form a core-shell like structure. First of all, the crystal size of Na/SSZ-13 is controlled by adding different number of seed crystals in the process of synthesizing SSZ-13. Following with the template removed from Na/SSZ-13, NH_4/SSZ-13 was obtained by twice ion-exchanging with 0.1 mol/L NH_4NO_3. Then NH_4/SSZ-13 was ion-exchanged by 0.1 mol/L Cu $(NO_3)_2$ to prepare Cu/SSZ-13.The results showed that larger the crystal size of molecular sieve catalysts, more favorable the distribution of Cu in the crystal core, and reduce the possibility to be replaced by Na to form CuO [175]. Zhang *et al.* found an MnO_x octahedral molecular sieve catalyst which had an alkali metal capture site can possess excellent alkali metal resistance (Fig. 7) [176,177]. Therefore, the method of separating the activated sites from the alkali metal sites can also be used to enhance the ability to resist alkali metal poisoning of molecular sieve catalysts.

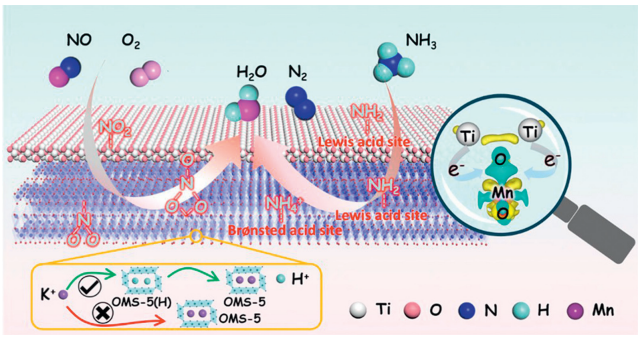

Fig. 7. Schematic diagram of the promotional effects of Fe doped OMS-2 catalysts. Reproduced with permission [177]. Copyright 2019, American Chemical Society.

5. Deactivation mechanism and anti-deactivation strategies for hydrocarbon poisoning

5.1. Deactivation mechanism for hydrocarbon poisoning

Because of the incomplete combustion of fuel, there are some hydrocarbons (HC) in the diesel exhaust, which will also influence the NO_x reduction ability of molecular sieve catalysts. Kim *et al.* proposed that C_3H_6 can inhibit the reaction between NO_x and feed NH_3, thus reducing the conversion rate of NO_x [178]. Some studies have shown that under standard SCR conditions, C_3H_6 has a great inhibition on the catalytic performance of Cu-zeolite catalysts. This deactivation mechanism is not raised from the competitive adsorption of C_3H_6 and NH_3, but from some intermediate species formed on surface during C_3H_6 oxidation [179]. Acrolein and coke, for example, would significantly mask the copper sites, thereby reducing catalyst performance. In addition, C_3H_6 will quickly reduce NO_2 to NO, affecting the process of fast SCR reaction. Some researchers proposed that the influence of hydrocarbons on Fe-zeolite catalysts was greater than that of Cu-zeolites [180]. He *et al.* found that the introduction of C_3H_6 would not only lead to coke deposition on Fe/Beta catalyst, but also result in partial reduction of Fe^{2+}, thereby reducing NH_3-SCR activity of Fe/Beta [181]. In addition, the blockage of channels and Fe sites caused by the deposition of intermediate products, the competitive adsorption with ammonia and the unnecessary consumption of NH_3 caused by secondary reactions are all reasons for the decreased SCR activity after hydrocarbon poisoning of Fe-zeolite catalyst [182–184].

5.2. Anti-deactivation strategies for hydrocarbon poisoning

The effect of hydrocarbons on molecular sieve catalysts depends in part on the pore structure. Porous molecular sieve catalysts can prevent the diffusion of long chain HCs molecules to the internal active center, which can effectively reduce the deposition of coke and relieve the influence of HCs on catalyst [185]. Therefore, the problem of HCs poisoning can be dealt with by selecting molecular sieve catalysts with small pores. In addition, general strategies to hence the anti-poisoning ability of molecular sieve catalysts, like adding additives and constructing core-shell structure can also be used. Cao *et al.* introduced Y into Cu-SAPO-34 and found that the addition of Y not only efficiently promoted the copper dispersion, enhanced the acid density, increased separated copper ions, but also reduced the adsorption of C_3H_6 [186]. The addition of Ce can also play a role in strengthening the HCs resistance of molecular sieve catalysts [187,188]. The meso–Cu-SSZ-13@mesoporous aluminosilicate catalyst with a core-shell structure constructed by Zhang *et al.* also had the excellent propylene resistance (Fig. S11 in Supporting information) [189]. Recently, Zang *et al.* reported that Cu-ZK-5 catalysts with different copper loadings exhibited significantly

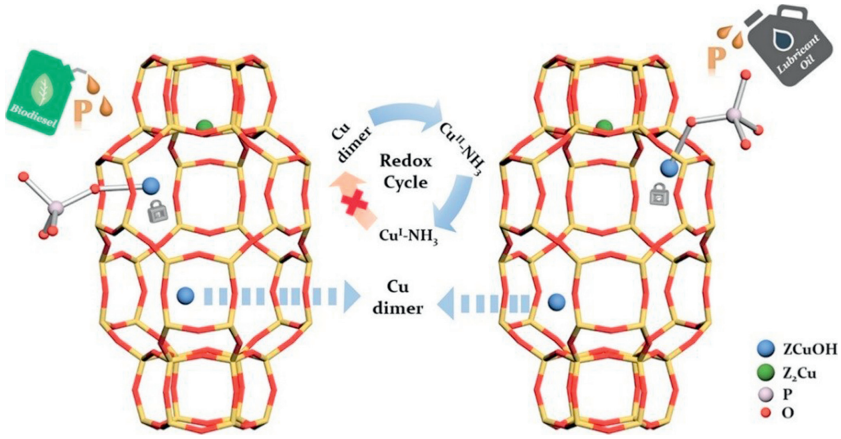

Fig. 8. Deactivation mechanism of Cu-SSZ-13 catalyst by phosphorus. Reproduced with permission [197]. Copyright 2021, American Chemical Society.

different catalytic performance of NH_3-SCR and also expressed excellent resistance to propylene poisoning. The $Cu_{7.55}$-ZK-5 catalyst with appropriate copper loading owned a large amount of isolated Cu^{2+}, which was conducive to the adsorption and activation of NO_x. In addition, the $Cu_{7.55}$-ZK-5 catalyst also exhibited a strong oxidation effect on propene, in which the propene can be completely oxidized at medium and high temperature [190].

6. Deactivation mechanism and anti-deactivation strategies for phosphorus poisoning

Phosphorus in mobile exhaust is mainly brought by fuel and lubricating oil, which will cause severe deactivation of molecular sieve catalysts. According to research, the activity of Fe/zeolite catalysts damaged severely when exposed to phosphate [171,191]. Of course, the Cu-zeolite catalyst will inevitably be affected by P species. In the early stage, Andonova *et al.* studied the influence of poisoning temperature and phosphorus concentration in the feed on the inactivation of Cu/BEA catalyst. It was observed that the pore condensation of H_3PO_4, the pore blockage and copper phosphate formation all resulted in the decrease of active copper species. These physical and chemical deactivation jointly affected the NH_3-SCR efficiency of molecular sieve catalysts [192]. The phosphorus poisoning mechanism on commercial Cu-SSZ-13 catalysts has been explored systematically. It is known that phosphate will be deposited in the pore, resulting in the blockage of the pore of the Cu-SSZ-13 catalyst, covering the acidic sites of the catalyst. And copper phosphate will be generated in the large cage of the molecular sieve, which will lead to the decrease of active Cu sites and the redox ability [193–196]. Recently, Guo *et al.* have also made some new discoveries about phosphorus deactivation mechanism of Cu-SSZ-13 (Fig. 8). They reported the strong interaction between Cu and P in the NH_3-SCR process at low temperature, which not only reduced the active site of Cu, but also restricted the dynamic movement of Cu. In addition, P poisoning can also significantly affect the redox cycling of $Cu^{II} \leftrightarrow Cu^{I}$ at Cu sites, particularly the $Cu^{I} \rightarrow Cu^{II}$ reoxidation half-cycle, because P poisoning could inhibit the formation of vital dimer Cu intermediates [197].

Besides, phosphorus can also combine with aluminum in the molecular sieve framework to form $AlPO_x$ species. Compared with fresh catalysts, the dealuminization of Cu-SSZ-13 poisoned by P was more serious after hydrothermal aging (Fig. S12 in Supporting information), indicating that P led to the decrease of the thermal stability [194,198].

The effect of phosphorus on NH_3-SCR catalysts is not absolute, and poisoning in the form of phosphate will lead to the decrease of catalyst activity. However, if phosphorylation is adopted, or phosphorus is introduced into the zeolite catalyst as a modifier, the performance of catalyst can be improved (Fig. S13 in Supporting information) [199–201]. In the actual working condition, phosphorus oxide (P_2O_5), partial phosphate (PO_3^-) and phosphate (PO_4^{3-}) are formed on the poisoning catalyst surface, among which partial phosphate is the main compound, so it will have a toxic effect on catalysts [194]. It has been concluded that the Cu-zeolite catalysts are more sensitive to phosphorus poisoning than to alkali and alkaline earth metals. However, there are still few strategies that can solve this problem. Chen *et al.* regenerated the phosphorus-poisoned Cu-SSZ-13 catalyst by hot water washing. In short, 1 g of the phosphated Cu-SSZ-13 catalyst was mixed with 100 g of deionized water. Then, the suspension was stirred and refluxed at 90 °C for a few days. After separation, washing with deionized water, and drying at 110 °C, the regenerated Cu-SSZ-13 catalyst was obtained. It was found that after regeneration, the recovery of the decreased accessibility and porosity, the deactivated Brønsted acid site and the recovery of Cu^{2+} ions can restore the activity and hydrothermal stability of poisoned Cu-SSZ-13 catalysts, which provides an effective method for extending the lifetime of Cu-SSZ-13 catalysts in practical application [202]. Chen *et al.* revealed that phosphorus poisoning significantly decreased the low-temperature NH_3-SCR catalytic activity, however, such activity loss was alleviated by further hydrothermal aging treatment. It was found that Cu-P species produced by phosphorus poisoning decreased the redox ability of active copper species, resulting in the observed low-temperature deactivation. And Cu-P species could partly decompose with the formation of active CuO_x species and a release of active copper species after hydrothermal aging treatment [203]. It remains to be studied in the future to improve the phosphorus toxicity resistance of other molecular sieve catalysts.

7. Summary and outlook

In summary, molecular sieve catalysts have large specific surface area, unique and regular pore structure, and abundant exchangeable Brønsted acid sites. Industrial Cu exchange microporous molecular sieve catalysts, like Cu-SSZ-13 or Cu-SAPO-34 have been used for the NO_x reduction in mobile exhaust gasses for nearly ten years. These zeolite catalysts are active in a wide active temperature window and are resistant to high-temperature dealumination. However, they still faced many challenges including hydrothermal aging, SO_2 poisoning, alkali-metal poisoning, HCs poisoning and phosphorus poisoning deactivation [204,205]. Among them, hydrothermal aging is the most serious problem faced by molecular

sieve catalysts at present, which needs to be solved urgently. In addition, other situations like HCl poisoning and Pt poisoning may also affect the activity of molecular sieve catalysts [206,207]. However, currently, the deactivation mechanism of molecular sieve catalysts is mainly studied in the above aspects. By summarizing the related researches, we can classify the deactivation mechanisms of hydrothermal aging or various toxic substances to catalysts as (1) the effect on catalyst structure, (2) the effect on active species, and (3) the effect on catalyst surface properties. These factors greatly damage the catalyst by reducing the adsorption of NH_3 or NO_x species, affecting or cutting off the reaction path, thus greatly impairing NO_x reduction performance. The toxic substances would also react with the feed gas to produce inert intermediate species, which covers the active sites of catalysts and lead to the useless consumption of NH_3. At present, the anti-deactivation strategies proposed to solve these problems of molecular sieve catalysts can also be concluded as follows: (1) adding additives, (2) constructing core-shell structure, (3) adjusting preparation methods and (4) exploring novel topological structures. These strategies can mitigate the deactivation of catalysts by establishing sacrifice sites and protective layer. However, these methods cannot solve all problems, such as P poisoning, and so far, there are few solutions other than hot water washing. These related studies show that molecular sieve catalysts are one of vital commercial catalysts with unique advantages and they are difficult to be replaced. Therefore, the research on mobile source catalysts is still based on further promote the NO_x reduction performance and achieve some deactivation issues of molecular sieve catalysts. In this paper, we briefly reviewed the deactivation mechanisms of molecular sieve catalysts, hoping to provide convenience for researchers to understand the various deactivation mechanisms of catalysts, so as to propose more effective anti-deactivation strategies.

In addition, the composition of exhaust gasses is complex, and there may be many factors affecting the activity of de-NO_x catalyst. For example, as for metal oxide catalysts, many reports have studied the deactivation mechanism of catalysts after multiple deactivation and anti-deactivation strategies [5,15,16,21,63,208]. Zou *et al.* unraveled the unanticipated differential compensated or aggravated Pb and SO_2 copoisoning effects over ceria-based catalysts for NO_x reduction and provided effective solutions to design ceria-based SCR catalysts with remarkable copoisoning resistance for the coexistence of heavy metals and SO_2. So molecular sieve catalyst in the application also face the same problem [5]. However, most studies on the deactivation of molecular sieve catalysts only consider one factor, and few studies report the influence of two and more factors together, such as SO_2&P, K&P or SO_2&hydrothermal aging [209]. There is a lack of research on the effects of the simultaneous existence of multiple poisons. There may be some interactions among various poisoning factors. The study and understanding of various poisoning mechanisms and the interaction between different toxic substance will be more conducive to the promotion of molecular sieve catalysts in the future. Therefore, the study on the simultaneous poisoning of multiple elements should be an important research filed of molecular sieve catalysts. Besides, for some unresolved poisoning problems, more efforts should be devoted to exploring innovative anti-deactivation strategies. Some researchers also mentioned that the high preparation cost of molecular sieve catalysts has greatly limited its wide application. Therefore, we need to synthesis molecular sieve catalysts from the perspective of low preparation cost, so as to maximize to advantages of molecular sieve catalysts and further reduce NO_x emissions.

Declaration of competing interest

All authors declare that there are no conflicts of interest, financial or otherwise in this work, and there are no other relationships or activities that can appear to have influenced the submitted work.

Acknowledgments

All authors acknowledge the support from the National Natural Science Foundation of China (No. 22125604), and the Chenguang Program supported by Shanghai Education Development Foundation and Shanghai Municipal Education Commission (No. 22Z00354).

Supplementary materials

Supplementary material associated with this article can be found, in the online version, at doi:10.1016/j.cclet.2023.108800.

References

[1] P. Forzatti, I. Nova, E. Tronconi, Angew. Chem. Int. Ed. 48 (2009) 8366–8368.
[2] L. Han, S. Cai, M. Gao, et al., Chem. Rev. 119 (2019) 10916–10976.
[3] S.C. Anenberg, J. Miller, R. Minjares, et al., Nature 545 (2017) 467–471.
[4] P. Zhang, A. Chen, T. Lan, et al., J. Hazard. Mater. 441 (2023) 129867.
[5] J. Zou, S. Impeng, F. Wang, et al., Environ. Sci. Technol. 56 (2022) 13368–13378.
[6] X. Zhou, P. Wang, Z. Shen, et al., Chem. Eng. J. 442 (2022) 136182.
[7] F. Wang, P. Wang, T. Lan, et al., ACS Catal. 12 (2022) 7622–7632.
[8] J. Song, S. Impeng, J. Zhang, et al., J. Catal. 416 (2022) 198–208.
[9] Z. Xu, S. Impeng, X. Jia, et al., Environ. Sci. Nano 9 (2022) 2121–2133.
[10] C. Feng, L. Han, P. Wang, et al., J. Environ. Sci. 111 (2022) 340–350.
[11] G. He, Z. Lian, Y. Yu, et al., Sci. Adv. 4 (2018) eaau4637.
[12] Christopher Paolucci, et al., Science 357 (2017) 898–903.
[13] L. Ye, P. Lu, D. Chen, et al., Chin. Chem. Lett. 32 (2021) 2509–2512.
[14] H. Wang, T. Zhu, Y. Qiao, et al., Chin. Chem. Lett. 33 (2022) 5223–5227.
[15] P. Zhang, P. Wang, S. Impeng, et al., Environ. Sci. Technol. 56 (2022) 12553–12562.
[16] Z. Shen, X. Liu, S. Impeng, et al., Environ. Sci. Technol. 56 (2022) 5141–5149.
[17] X. Qi, L. Han, J. Deng, et al., Environ. Sci. Technol. 56 (2022) 5840–5848.
[18] M. Lyu, J. Zou, X. Liu, et al., Catal. Sci. Technol. 12 (2022) 4020–4031.
[19] S. Li, W. Hu, Z. Xu, et al., ChemCatChem 14 (2022) e202200476.
[20] W. Hu, J. He, X. Liu, et al., Environ. Sci. Technol. 56 (2022) 5170–5178.
[21] L. Yan, F. Wang, P. Wang, et al., Environ. Sci. Technol. 54 (2020) 7697–7705.
[22] C. Negri, T. Selleri, E. Borfecchia, et al., J. Am. Chem. Soc. 142 (2020) 15884–15896.
[23] C. Paolucci, A.A. Parekh, I. Khurana, et al., J. Am. Chem. Soc. 138 (2016) 6028–6048.
[24] A.M. Beale, F. Gao, I. Lezcano-Gonzalez, et al., Chem. Soc. Rev. 44 (2015) 7371–7405.
[25] C.W. Andersen, E. Borfecchia, M. Bremholm, et al., Angew. Chem. Int. Ed. 56 (2017) 10367–10372.
[26] J. Wang, H. Zhao, G. Haller, Y. Li, Appl. Catal. B 202 (2017) 346–354.
[27] N.H. Ahn, T. Ryu, Y. Kang, et al., ACS Catal. 7 (2017) 6781–6785.
[28] D. Jo, T. Ryu, G.T. Park, et al., ACS Catal. 6 (2016) 2443–2447.
[29] J. Dickson, N.A. Conroy, Y. Xie, et al., Chem. Eng. J. 402 (2020) 126268.
[30] D. Yuan, C. Kang, W. Wang, et al., Catal. Sci. Technol. 6 (2016) 8364–8374.
[31] W. Cui, D. Zhu, J. Tan, et al., Chin. J. Catal. 43 (2022) 1945–1954.
[32] J. Grand, S.N. Talapaneni, A. Vicente, et al., Nat. Mater. 16 (2017) 1010–1015.
[33] X. Shen, W. Mao, Y. Ma, et al., Angew. Chem. Int. Ed. 57 (2018) 724–728.
[34] B. Min, S. Yang, A. Korde, et al., Angew. Chem. Int. Ed. 58 (2019) 8201–8205.
[35] C. Wang, W. Fang, Z. Liu, et al., Nat. Nanotechnol. 17 (2022) 714–720.
[36] S. Yang, C. Yu, L. Yu, et al., Angew. Chem. Int. Ed. 56 (2017) 12553–12556.
[37] P.S. Huang, C.H. Lam, C.Y. Su, et al., Angew. Chem. Int. Ed. 57 (2018) 13271–13276.
[38] G. Sun, R. Yu, L. Xu, et al., Catal. Sci. Technol. 12 (2022) 3898–3911.
[39] P. Xiao, Y. Wang, Y. Lu, et al., Appl. Catal. B 325 (2023) 122395.
[40] M.H. Mahyuddin, A. Staykov, Y. Shiota, et al., ACS Catal. 7 (2017) 3741–3751.
[41] E. Bello-Jurado, D. Schwalbe-Koda, M. Nero, et al., Angew. Chem. Int. Ed. 61 (2022) e202201837.
[42] M. Salazar, S. Hoffmann, O.P. Tkachenko, et al., Appl. Catal. B 182 (2016) 213–219.
[43] M. Salazar, R. Becker, W. Grünert, Appl. Catal. B 165 (2015) 316–327.
[44] N.C. Nelson, T. Andana, K.G. Rappé, Y. Wang, Catal. Sci. Technol. 13 (2023) 1111–1118.
[45] R. Yu, Z. Zhao, S. Huang, W. Zhang, Appl. Catal. B 269 (2020) 118825.
[46] F. Gao, D. Mei, Y. Wang, et al., J. Am. Chem. Soc. 139 (2017) 4935–4942.
[47] C. Paolucci, A.A. Verma, S.A. Bates, et al., Angew. Chem. Int. Ed. 53 (2014) 11828–11833.
[48] A. Wang, Y. Chen, E.D. Walter, et al., Nat. Commun. 10 (2019) 1137.
[49] W. Su, H. Chang, Y. Peng, et al., Environ. Sci. Technol. 49 (2015) 467–473.
[50] Z. Chen, C. Bian, C. Fan, T. Li, Chin. Chem. Lett. 33 (2022) 893–897.
[51] R. Martínez-Franco, M. Moliner, J.R. Thogersen, A. Corma, ChemCatChem 5 (2013) 3316–3323.

[52] X. Xiang, M. Yang, B. Gao, et al., RSC Adv. 6 (2016) 12544–12552.
[53] P. Concepción, M. Boronat, R. Millán, et al., Top. Catal. 60 (2017) 1653–1663.
[54] E. Yuan, G. Wu, W. Dai, et al., Catal. Sci. Technol. 7 (2017) 3036–3044.
[55] Y. Naraki, K. Ariga, T. Sano, Adv. Porous Mater. 4 (2016) 125–133.
[56] N. Zhu, Z. Lian, Y. Zhang, et al., Chin. Chem. Lett. 30 (2019) 867–870.
[57] T. Ryu, N.H. Ahn, S. Seo, et al., Angew. Chem. Int. Ed. 56 (2017) 3256–3260.
[58] C. Yu, L. Dong, F. Chen, et al., Environ. Technol. 38 (2017) 1030–1042.
[59] M. Chen, Q. Sun, X. Yang, J. Yu, Inorg. Chem. Commun. 105 (2019) 203–207.
[60] A. Sultana, M. Sasaki, K. Suzuki, H. Hamada, Catal. Commun. 41 (2013) 21–25.
[61] T.K.R. de Oliveira, M. Rosset, O.W. Perez-Lopez, Catal. Commun. 104 (2018) 32–36.
[62] P. Zhang, P. Wang, A. Chen, et al., Environ. Sci. Technol. 55 (2021) 11970–11978.
[63] S. Cai, T. Xu, P. Wang, et al., Environ. Sci. Technol. 54 (2020) 12752–12760.
[64] W. Hu, Y. Zhang, S. Liu, et al., Appl. Catal. B 206 (2017) 449–460.
[65] Y. Peng, W. Si, X. Li, et al., Environ. Sci. Technol. 50 (2016) 9576–9582.
[66] P.S. Hammershøi, Y. Jangjou, W.S. Epling, et al., Appl. Catal. B 226 (2018) 38–45.
[67] P.S. Hammershøi, P.N.R. Vennestrøm, H. Falsig, et al., Appl. Catal. B 236 (2018) 377–383.
[68] Y. Jangjou, Q. Do, Y. Gu, et al., ACS Catal. 8 (2018) 1325–1337.
[69] V.V. Mesilov, S.L. Bergman, S. Dahlin, et al., Appl. Catal. B 284 (2021) 119756.
[70] L. Wei, D. Yao, F. Wu, et al., Ind. Eng. Chem. Res. 58 (2019) 3949–3958.
[71] Y. Zhang, Y. Peng, J. Li, et al., ACS Catal. 10 (2020) 9410–9419.
[72] Y.J. Kim, J.K. Lee, K.M. Min, et al., J. Catal. 311 (2014) 447–457.
[73] J. Luo, D. Wang, A. Kumar, et al., Catal. Today 267 (2016) 3–9.
[74] S. Han, Q. Ye, S. Cheng, et al., Catal. Sci. Technol. 7 (2017) 703–717.
[75] P. Wang, L. Yan, Y. Gu, et al., Environ. Sci. Technol. 54 (2020) 6396–6405.
[76] F. Gao, Y. Wang, N.M. Washton, et al., ACS Catal. 5 (2015) 6780–6791.
[77] Y. Cui, Y. Wang, D. Mei, et al., J. Catal. 378 (2019) 363–375.
[78] J.H. Kwak, D. Tran, S.D. Burton, et al., J. Catal. 287 (2012) 203–209.
[79] L. Ma, Y. Cheng, G. Cavataio, et al., Chem. Eng. J. 225 (2013) 323–330.
[80] D. Wang, Y. Jangjou, Y. Liu, et al., Appl. Catal. B 165 (2015) 438–445.
[81] F. Gao, J. Szanyi, Appl. Catal. A 560 (2018) 185–194.
[82] M. Valdez Lancinha Pereira, A. Nicolle, D. Berthout, Catal. Today 258 (2015) 424–431.
[83] W. Su, Z. Li, Y. Peng, J. Li, Phys. Chem. Chem. Phys. 17 (2015) 29142–29149.
[84] D. Fan, J. Wang, T. Yu, et al., Chem. Eng. Sci. 176 (2018) 285–293.
[85] J. Tang, M. Xu, T. Yu, et al., Chem. Eng. Sci. 168 (2017) 414–422.
[86] L. Wang, J.R. Gaudet, W. Li, D. Weng, J. Catal. 306 (2013) 68–77.
[87] X. Liu, X. Wu, D. Weng, et al., Catal. Today 281 (2017) 596–604.
[88] P.N.R. Vennestrøm, T.V.W. Janssens, A. Kustov, et al., J. Catal. 309 (2014) 477–490.
[89] S. Brandenberger, O. Kröcher, M. Casapu, et al., Appl. Catal. B 101 (2011) 649–659.
[90] L. Kovarik, N.M. Washton, R. Kukkadapu, et al., ACS Catal. 7 (2017) 2458–2470.
[91] S. Shwan, J. Jansson, J. Korsgren, et al., Catal. Today 197 (2012) 24–37.
[92] S. Shwan, R. Nedyalkova, J. Jansson, et al., Ind. Eng. Chem. Res. 51 (2012) 12762–12772.
[93] M. Iwasaki, K. Yamazaki, H. Shinjoh, Appl. Catal. B 102 (2011) 302–309.
[94] Q. Lin, X. Feng, H. Zhang, et al., J. Ind. Eng. Chem. 65 (2018) 40–50.
[95] M. Iwasaki, H. Shinjoh, Chem. Commun. 47 (2011) 3966–3968.
[96] J. Wang, Z. Peng, H. Qiao, et al., Ind. Eng. Chem. Res. 55 (2016) 1174–1182.
[97] T. Usui, Z. Liu, S. Ibe, et al., ACS Catal. 8 (2018) 9165–9173.
[98] Z. Zhao, R. Yu, C. Shi, et al., Catal. Sci. Technol. 9 (2019) 241–251.
[99] L. Gao, W. Gao, H. Wang, et al., Chem. Eng. J. 455 (2023) 140520.
[100] M. Chen, W. Zhao, Y. Wei, et al., Nano Res. (2023), doi:10.1007/s12274-023-5500-x.
[101] D. Deng, S. Deng, D. He, et al., J. Rare Earths 39 (2021) 969–978.
[102] B. Guan, H. Jiang, X. Peng, et al., Appl. Catal. A 617 (2021) 118110.
[103] X. Xiang, Y. Cao, L. Sun, et al., Appl. Catal. A 551 (2018) 79–87.
[104] Z. Zhao, R. Yu, R. Zhao, et al., Appl. Catal. B 217 (2017) 421–428.
[105] H. Zhao, Y. Zhao, M. Liu, et al., Appl. Catal. B 252 (2019) 230–239.
[106] L. Wang, Y. Shao, J. Zhang, M. Anpo, Micropor. Mesopor. Mater 95 (2006) 17–25.
[107] H. Tian, Y. Ping, Y. Zhang, et al., J. Hazard. Mater. 416 (2021) 126194.
[108] H. Jiang, B. Guan, X. Peng, et al., Chem. Eng. J. 379 (2020) 122358.
[109] Y. Ma, H. Zhao, C. Zhang, et al., Catal. Today 355 (2020) 627–634.
[110] H. Zhao, Y. Zhao, Y. Ma, et al., J. Catal. 377 (2019) 218–223.
[111] L. Wang, J. Zhang, F. Chen, Micropor. Mesopor. Mater 122 (2009) 229–233.
[112] S. Huang, J. Wang, J. Wang, et al., Appl. Catal. B 248 (2019) 430–440.
[113] Y. Zhang, H. Wang, R. Chen, RSC Adv. 5 (2015) 67841–67848.
[114] T. Zhang, J. Shi, J. Liu, et al., Appl. Surf. Sci. 375 (2016) 186–195.
[115] M. Chen, Q. Sun, G. Yang, et al., ChemCatChem 11 (2019) 3865–3870.
[116] X. Wang, M. Qin, Y. Xu, Q. Li, J. Colloid Interface Sci. 638 (2023) 686–694.
[117] H. Pu, C. Han, H. Wang, et al., Appl. Surf. Sci. 258 (2012) 8895–8901.
[118] T. Jiang, D. Wu, J. Song, et al., Powder Technol 207 (2011) 422–427.
[119] J. Xu, W. Chu, S. Luo, J. Mol. Catal. A 256 (2006) 48–56.
[120] L. Wang, J. Zhang, F. Chen, M. Anpo, J. Phys. Chem. C 111 (2007) 13648–13651.
[121] J. Xu, Q. Zhang, F. Guo, et al., New J. Chem. 42 (2018) 19000–19007.
[122] Y.M. Luo, Z.Y. Hou, D.F. Jin, X.M. Zheng, Chin. J. Chem. 25 (2007) 635–639.
[123] C.F. Cheng, S.H. Chou, P.W. Cheng, et al., J. Chin. Chem. Soc. 54 (2007) 35–40.
[124] C. Han, H. Wang, L. Zhang, et al., Adv. Powder Technol. 22 (2011) 20–25.
[125] M. Moliner, C. Franch, E. Palomares, et al., Chem. Commun. 48 (2012) 8264–8266.
[126] Y. Shan, W. Shan, X. Shi, et al., Appl. Catal. B 264 (2020) 118511.
[127] T. Ryu, Y. Kang, I.S. Nam, S.B. Hong, React. Chem. Eng. 4 (2019) 1050–1058.
[128] J. Zhu, Z. Liu, K. Iyoki, et al., Chem. Commun. 53 (2017) 6796–6799.
[129] M. De Prins, E. Verheyen, S. Kerkhofs, et al., Chem. Commun. 54 (2018) 5626–5629.
[130] T. Takata, N. Tsunoji, Y. Takamitsu, et al., Micropor. Mesopor. Mater. 225 (2016) 524–533.
[131] A. Wang, P. Arora, D. Bernin, et al., Appl. Catal. B 246 (2019) 242–253.
[132] J. Wan, H. Yang, Y. Shi, et al., J. Environ. Sci. 126 (2023) 445–458.
[133] Y. Shan, J. Du, Y. Zhang, et al., Natl. Sci. Rev. 8 (2021) nwab010.
[134] P.S. Hammershøi, A.D. Jensen, T.V.W. Janssens, Appl. Catal. B 238 (2018) 104–110.
[135] D.W. Brookshear, J.G. Nam, K. Nguyen, et al., Catal. Today 258 (2015) 359–366.
[136] W. Su, Z. Li, Y. Zhang, et al., Catal. Sci. Technol. 7 (2017) 1523–1528.
[137] S.L. Bergman, S. Dahlin, V.V. Mesilov, et al., Appl. Catal. B 269 (2020) 118722.
[138] P.S. Hammershøi, A.L. Godiksen, S. Mossin, et al., React. Chem. Eng. 4 (2019) 1081–1089.
[139] A.J. Shih, I. Khurana, H. Li, et al., Appl. Catal. A 574 (2019) 122–131.
[140] S. Dahlin, C. Lantto, J. Englund, et al., Catal. Today 320 (2019) 72–83.
[141] K. Wijayanti, K. Xie, A. Kumar, et al., Appl. Catal. B 219 (2017) 142–154.
[142] K. Wijayanti, K. Leistner, S. Chand, et al., Catal. Sci. Technol. 6 (2016) 2565–2579.
[143] K. Wijayanti, S. Andonova, A. Kumar, et al., Appl. Catal. B 166-167 (2015) 568–579.
[144] G. Yang, X. Du, J. Ran, et al., J. Phys. Chem. C 122 (2018) 21468–21477.
[145] X. Liu, X. Wu, D. Weng, Z. Si, Catal. Commun. 59 (2015) 35–39.
[146] M. Shen, H. Wen, T. Hao, et al., Catal. Sci. Technol. 5 (2015) 1741–1749.
[147] L. Zhang, D. Wang, Y. Liu, et al., Appl. Catal. B 156-157 (2014) 371–377.
[148] Y. Jangjou, M. Ali, Q. Chang, et al., Catal. Sci. Technol. 6 (2016) 2679–2685.
[149] C. Wang, J. Wang, J. Wang, et al., Appl. Catal. B 204 (2017) 239–249.
[150] Y. Jangjou, D. Wang, A. Kumar, et al., ACS Catal. 6 (2016) 6612–6622.
[151] J. Du, X. Shi, Y. Shan, et al., Catal. Sci. Technol. 10 (2020) 1256–1263.
[152] X. Liu, X. Wu, D. Weng, et al., RSC Adv. 7 (2017) 37787–37796.
[153] J. He, S. Impeng, J. Zhang, et al., Chem. Eng. J. 448 (2022) 137720.
[154] Y. Fan, W. Ling, B. Huang, et al., J. Ind. Eng. Chem. 56 (2017) 108–119.
[155] L. Jun, J. Liwei, J. Weiyang, et al., Rare Metal Mat. Eng. 44 (2015) 1612–1616.
[156] Y. Li, W. Song, J. Liu, et al., Chem. Eng. J. 330 (2017) 926–935.
[157] C. Yu, B. Huang, L. Dong, et al., Chem. Eng. J. 316 (2017) 1059–1068.
[158] C. Peng, R. Yan, H. Peng, et al., J. Hazard. Mater. 385 (2020) 121593.
[159] J. He, J. Deng, J. Zhang, et al., Catal. Sci. Technol. 13 (2023) 2480–2492.
[160] X. Chen, Y. Geng, W. Shan, F. Liu, Ind. Eng. Chem. Res. 57 (2018) 1399–1407.
[161] R.T. Guo, S.X. Wang, W.G. Pan, et al., J. Phys. Chem. C 121 (2017) 7881–7891.
[162] S.S.R. Putluru, A. Riisager, R. Fehrmann, Appl. Catal. B 101 (2011) 183–188.
[163] S.S.R. Putluru, A.D. Jensen, A. Riisager, R. Fehrmann, Catal. Commun. 18 (2012) 41–46.
[164] J. Ma, Z. Si, D. Weng, et al., Chem. Eng. J. 267 (2015) 191–200.
[165] L. Liu, X. Wu, Y. Ma, et al., Chem. Eng. J. 383 (2020) 123080.
[166] C. Wang, C. Wang, J. Wang, et al., J. Environ. Sci. 70 (2018) 20–28.
[167] H. Xue, X. Guo, S. Wang, et al., Catal. Commun. 112 (2018) 53–57.
[168] C. Fan, Z. Chen, L. Pang, et al., Chem. Eng. J. 334 (2018) 344–354.
[169] N. Zhu, W. Shan, Y. Shan, et al., Chem. Eng. J. 388 (2020) 124250.
[170] S. Ming, L. Pang, C. Fan, et al., Chin. J. Catal. 40 (2019) 590–599.
[171] P. Kern, M. Klimczak, T. Heinzelmann, et al., Appl. Catal. B 95 (2010) 48–56.
[172] J. Liu, H. Cheng, H. Zheng, et al., ACS Catal. 11 (2021) 14727–14739.
[173] S. Shwan, J. Jansson, L. Olsson, M. Skoglundh, Appl. Catal. B 166-167 (2015) 277–286.
[174] J. Liu, J. Liu, Z. Zhao, et al., Catal. Surv. Asia 22 (2018) 181–194.
[175] Z. Chen, M. Shen, C. Wang, et al., Catalysts 11 (2021) 979.
[176] K. Zha, C. Feng, L. Han, et al., Chem. Eng. J. 381 (2020) 122764.
[177] L. Yan, Y. Gu, L. Han, et al., ACS Appl. Mater. Interfaces 11 (2019) 11507–11517.
[178] M.Y. Kim, J.S. Choi, M. Crocker, Catal. Today 231 (2014) 90–98.
[179] J.Y. Luo, H. Oh, C. Henry, W. Epling, Appl. Catal. B 123-124 (2012) 296–305.
[180] T. Selleri, I. Nova, E. Tronconi, et al., Catal. Today 320 (2019) 100–111.
[181] C. He, Y. Wang, Y. Cheng, et al., Appl. Catal. A 368 (2009) 121–126.
[182] J. Li, R. Zhu, Y. Cheng, et al., Environ. Sci. Technol. 44 (2010) 1799–1805.
[183] X. Shi, H. He, L. Xie, Chin. J. Catal. 36 (2015) 649–656.
[184] I. Heo, Y. Lee, I.S. Nam, et al., Micropor. Mesopor. Mater. 141 (2011) 8–15.
[185] Q. Ye, L. Wang, R.T. Yang, Appl. Catal. A 427-428 (2012) 24–34.
[186] Y. Cao, X. Feng, H. Xu, et al., Catal. Commun. 76 (2016) 33–36.
[187] Y. Cao, L. Lan, X. Feng, et al., Catal. Sci. Technol. 5 (2015) 4511–4521.
[188] Y. Shi, X. Wang, Y. Xia, et al., Mol. Catal. 433 (2017) 265–273.
[189] T. Zhang, F. Qiu, J. Li, Appl. Catal. B 195 (2016) 48–58.
[190] Y. Zang, Y. Bi, C. Liu, et al., Fuel 340 (2023) 127442.
[191] S. Shwan, J. Jansson, L. Olsson, M. Skoglundh, Catal. Today 258 (2015) 432–440.
[192] K. Xie, A. Wang, J. Woo, et al., Appl. Catal. B 256 (2019) 117815.
[193] K. Xie, K. Leistner, K. Wijayanti, et al., Catal. Today 297 (2017) 46–52.
[194] K. Xie, J. Woo, D. Bernin, et al., Appl. Catal. B 241 (2019) 205–216.
[195] Z. Chen, C. Fan, L. Pang, et al., Appl. Catal. B 237 (2018) 116–127.
[196] S. Dahlin, J. Englund, H. Malm, et al., Catal. Today 360 (2021) 326–339.
[197] A. Guo, K. Xie, H. Lei, et al., Environ. Sci. Technol. 55 (2021) 12619–12629.
[198] A. Wang, K. Xie, D. Bernin, et al., Appl. Catal. B 269 (2020) 118781.
[199] H.E. van der Bij, B.M. Weckhuysen, Chem. Soc. Rev. 44 (2015) 7406–7428.
[200] Y. Yamasaki, N. Tsunoji, Y. Takamitsu, et al., Micropor. Mesopor. Mater. 223 (2016) 129–139.
[201] Y. Kakiuchi, T. Tanigawa, N. Tsunoji, et al., Appl. Catal. A 575 (2019) 204–213.

[202] Z. Chen, C. Bian, Y. Guo, et al., ACS Catal. 11 (2021) 12963–12976.
[203] J. Chen, Y. Shan, Y. Sun, et al., Environ. Sci. Technol. 57 (2023) 4113–4121.
[204] Q. Sun, N. Wang, J. Yu, Adv. Mater. 33 (2021) 2104442.
[205] Q. Zhang, S. Gao, J. Yu, Chem. Rev. 123 (2023) 6039–6106.
[206] J.W. Choung, I.S. Nam, Appl. Catal. A 312 (2006) 165–174.
[207] T. Yu, M. Xu, Y. Huang, et al., Appl. Catal. B 204 (2017) 525–536.
[208] L. Yan, Y. Ji, P. Wang, et al., Environ. Sci. Technol. 54 (2020) 9132–9141.
[209] Z. Liu, Y. Shan, S. Han, et al., Environ. Sci. Technol. 57 (2023) 4308–4317.